ICAS 2021 SHANGHAI
International Council of the Aeronautical Sciences
32nd Congress of the International Council of the Aeronautical Sciences
September 6-10, 2021
Pudong Shangri-La, Shanghai, China

ANALYSIS OF AERODYNAMIC COUPLING EFFECT IN CLOSE FORMATION FOR FLAPPING WINGS

Zhaotong Chen[1,2,3], Zongxia Jiao[1,2,3], Yaoxing Shang[1,2,3],Longfei Zhao[2,3,4]

[1]School of Automation Science and Electrical Engineering, Beihang University, Beijing 100191, China
[2]Science and Technology on Aircraft Control Laboratory, Beihang University, Beijing 100191, China
[3]Ningbo Institute of Technology, Beihang University, Ningbo 315800, China
[4]Research Institute for Frontier Science, Beihang University, 100191, Beijing, China

Abstract

This work explores the unsteady interaction between the streamwise vortices and the follower in a V-shaped close flapping wings formation. The advanced high fidelity LBM simulation and finite explicit dynamic solver are used to calculate the fluid structure interaction. First, the vortex effect during flapping process of flexible wing shows that the suction side adsorption effect after LEV formation will increase the lift. Due to the existence of angle of attack, the structure and aerodynamic characteristics of the LEV are different. In addition, the wing buffeting is caused by the breakdown of LEV near the median of stroke. Second, the flow structure is obviously different when the spatial phase is in phase. The spatial drift of follower's TIV, the delay of vortex shedding and the secondary vortex structure indicate that the coupling effect with incident vortex is strong. But in other temporal phases, these unsteady phenomena weaken or disappear, and are replaced by the finite time collision between the wing and the incident vortex. By comparing the aerodynamic load curves, it is found that the lift is significantly increased and the net thrust is decreased most in the same phase. However, this change is obviously weakened in other phases. The smaller the spatial phase difference is, the more obvious the aerodynamic effect is. This indicates that the coupling form of aerodynamic effect may exist between the close formation of flapping wing and the specific temporal phase when the position of two aircraft is fixed.

Keywords: wing-vortex-interaction, close formation, flapping wing, aerodynamics coupling

1. Introduction

For a long time, it has been considered that the formation flight of aircraft and birds has significant benefits to improve the aerodynamic performance. According to the distribution of aerodynamic force, the upwash flow generated by the tip vortex left behind by the tail of the front aircraft can be captured by properly positioning. The result is a forward inclined lift vector, which can increase the lift and reduce the induced drag, thus significantly saving energy [1]. Historically, safety concerns have limited close formation due to the high speed and close range of adjacent aircraft. Fortunately, technological advances in positioning and navigation systems and anti-collision systems have enabled military and commercial aircraft to fly closer, thus taking advantage of close formation flying. However, this is not without cost. Close formation flight can also produce adverse effects, including strong or unsteady vortex buffeting leading to structural fatigue or net upwash flow caused by improper position of wake vortex during capture [2]. Vortex capture is an elegant flow energy extraction mechanism, which has been used in nature and applied in engineering systems [3,4]. Therefore, it is important to understand the complex interaction between the streamwise vortices and the following wings for close formation.

We know that for fixed wing aircraft, according to the formation, development and breakdown of vortex wake, it can be divided into: Wake formation zone; stable wake zone; unstable wake zone; wake breakdown zone [5]. However, due to the complex unsteady aerodynamic mechanism of flapping wing, the development and properties of unsteady vortex generated by flapping wing are more special, which will gradually dissipate in several cycles after the wing falls off. Therefore, the aerodynamic coupling effect will be more prominent in close formation.

Many examples have the characteristics of flying in close formation. For example, migratory birds will move in a V-shape according to the seasonal migration, and many kinds of birds, such as pigeons,

fly in groups for certain production needs [6]. Although it is widely believed that the flight mode is not directly from the aerodynamics mechanism, researchers try to explore the theory and other evidence of formation and cluster flight of natural pilots. As early as 1970, Lissaman and Schollenberger used the classical aerodynamics theory to discuss the influence of the number, speed and Wingtip overlap of V-shaped bird formation on the induction power and flight efficiency [1]. They believed that when the number of birds in V-shaped formation reached 25 or more and the wingtip overlap among birds was certain, the power required for the lift of the whole formation could be reduced by 2.9 times, and the flight range could increase by about 70%. Henri Weimerskirch and colleagues [7] provided the first evidence of the energy efficiency of V-shaped formation flying. By using an implantable data recorder (a representative of energy consumption) that can record heart rate, they found that in a group of large white pelicans. The heart rate and wing beat frequency of the individuals flying in V-shaped formation were lower than those flying alone. Subsequently, the emergence of high-precision GPS observation technology provides an opportunity for later bird measurement with higher accuracy. In 2014, Portugal et al. [8] found that in formation flight, northern bald Ibis prefer fixed wing aerodynamics prediction position to obtain the best flight effect from the updraft, and can actively adjust the flapping phase to capture the upwash flow of the leader bird. This phase adjustment mechanism is in sharp contrast to the theory [9] that the flapping phase has no effect proposed by Lissaman et al. In other words, the discovery also emphasizes that the relationship between leader and follower is not only closely related in space, but also closely related to the phase change of their fight in time. Although these studies have made progress in the understanding, prediction and demonstration of tight formation flight benefits, further investigation is still needed before the flapping wing aircraft can achieve a feasible and safe tight formation flight capability.

The essence of aerodynamic coupling effect is a kind of interaction with the streamwise vortices generated by follower and leading aircraft, that is, the wing-vortex-interaction [10]. The interaction between streamwise vortex and aerodynamic surface will cause a wide range of unsteady phenomena which are difficult to predict, which will affect the drag and lift performance, as well as the unsteady load or buffeting experienced by the wing. It is expected that these effects will be crucial for the flapping wing formation with more compact and different configurations. For example, the strong and unfavorable local pressure gradient generated by vortex near the wing may lead to unstable separation on a part of the wing, which may lead to increased drag, reduced lift and unfavorable rolling torque, resulting in additional trim torque and further requirements on the control system. On the contrary, if the wing is in upwash / downwash flow induced by streamwise vortices, the effective angle of attack of the wing will be changed, thus affecting the development of leading-edge vortices and wingtip vortices, resulting in more complex unsteady aerodynamic phenomena, which will further affect the periodic characteristics of lift and drag distribution of the wing and change the aerodynamic efficiency of the formation. In addition, due to other factors, such as stability and control, and unpredictable wing vortex interaction, non-optimal formation can be observed in nature (large tip spacing, no phase locking, etc.).

However, whether it is fixed wing aircraft or flapping wings in nature, such wing vortex interaction does not need to be completely avoided, because it is likely that the improvement of aerodynamic efficiency will determine that the incident vortex needs to impact with the wing in some form of space, such as the lateral tip overlap of the follower and leader. Blake et al. conducted formation wind tunnel test [11-13] with delta wing aircraft without vertical tail, and found that the highest drag reduction rate of 25% was achieved when the overlap with follower was 15% - 20%. In Lissaman's research, it is believed that the aerodynamic efficiency of the following bird will reach the highest when there is a certain overlap of wingtips. In the long-distance migration of Ibis birds, the overlap degree of natural selection of birds' wingtips is also consistent with the prediction range of fixed wing aerodynamics. Therefore, the influence of the spatial relationship between the incident vortex and the wing on the aerodynamic force needs to be further discussed.

Another unsolved key problem is the flapping phase relationship between follower and leader. Different from the wake distribution of fixed wing aircraft, the vortex distribution caused by periodic flapping of flapping wing has a high spatial correlation with the tip trajectory. Therefore, when the tip trajectory of the follower keeps a different specific phase difference from that of the leader, the induced effect of the incident vortex will make the wing of the follower subject to different

aerodynamic interference, and the change of aerodynamic characteristics will also determine which phase strategy should be used to adjust the formation attitude.

In this work, we will provide a preliminary study on the aerodynamic effects of the flow vortices and wing interaction in the close formation of flapping wings, which will lay a foundation for further study of aerodynamic coupling effects. High fidelity numerical method based on LBM and finite element method are used to simulate fluid structure interaction. The influence of vortex wake disturbance on flow structure and unsteady load is discussed and proposed for different phase difference between follower and leader.

2. Methodology

2.1 Aerodynamic solver

In this study, the interactional aerodynamic features between flapping wing and elevon are analyzed by numerical simulation. LBM (lattice Boltzmann method) is applied using a commercial LBM code: Next Limit Technologies' XFlow, which is specifically designed for applications in situations of highly transient flow fields and models with large-amplitude moving parts. In addition, the large eddy simulation (LES) method is used in XFlow turbulence model to capture the main structures of vortex, which is suitable for the convection structure analysis in this study.

2.2 Structural dynamics solver and fluid structure interaction

In the part of structural dynamics, the explicit dynamic solver of ABAQUS is mainly used. Explicit dynamics is a supplement to implicit dynamics, and analytical method is a very effective tool for solving a wide range of nonlinear structural mechanics problems.

The key part of any aeroelastic calculation is the precise coupling between the fluid and structural components of the model. According to the data transfer form, it can be divided into unidirectional fluid structure coupling and bidirectional fluid structure coupling. Because this paper focuses on the influence of eddy current and involves the precise interaction between wing and air, the two-way fluid structure coupling method is selected. The structure receives the load data from the fluid, while the fluid part receives the displacement, velocity and coordinate data of the structure.

3. Details of the computations

3.1 Geometric definitions

As shown in Figure 1 (a), the effect of vortices is studied in a symmetric V-shaped flapping wing formation with Reynolds number Re = 20000. Each wing in the calculation is fan-shaped in plane, the leading-edge and the fixed bar in the figure are set as rigid, and the relative position of the two remains unchanged in flapping. The flexible PP film is used to simulate the passive torsion of flexible wing in flapping. In addition, a carbon fiber rod is embedded in the middle of the wing surface to improve the aerodynamic characteristics of the flapping wing aircraft. The flapping frequency is 10Hz, and the flapping angle changes with corresponding sine curve. The aspect ratio AR = b/C of flapping wing aircraft is 4, and the specifications of the two aircraft are exactly the same, and the uniform thickness is t/C = 0.002. The angle of attack is set to α = 10 ° relative to the free stream. According to the statistical law of the forward ratio of flapping wing organisms published in nature by Graham K. Taylor et al. [14], the free flow size is set as 2.5m/s^2, and the Strouhal number is St = 0.3. (These settings are based on the available flexible flapping wing platform to achieve the aerodynamic characteristics as close as possible to the real object.)

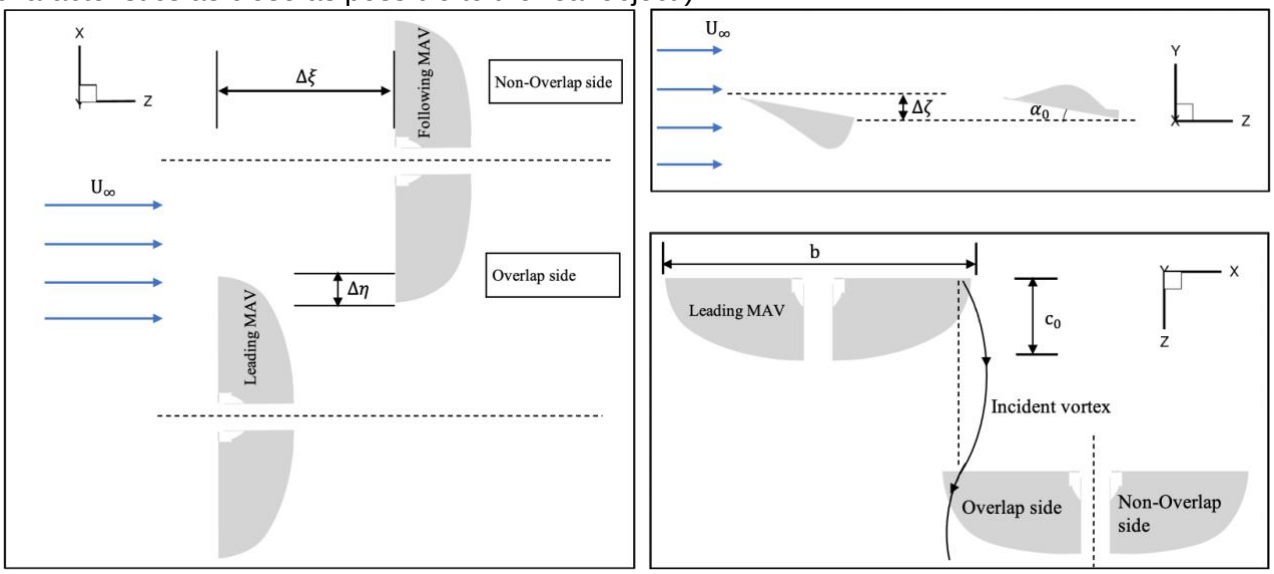

(a) Top view of wing formation arrangement. (c) Orientation of streamwise vortex.

Figure 1 – Configurations for close formation flight are shown in an (a) overhead view and (b) side view. Orientation of the incident vortex is demonstrated in (c) relative to a follower.

3.2 Formation configuration

In the aspect of formation geometry, several parameters define the position of the follower relative to the leader, such as the temporal phase $\phi_{temporal}$ which is used to characterize the temporal phase difference of the flapping and spatial phase $\phi_{spatial}$ which reflect the wavelength of two aircrafts. Also, $\Delta\xi$, $\Delta\eta$, $\Delta\zeta$ are used to measure the distance between the leading-edges of the two wings in streamwise, the overlap in the spanwise direction and the offset in the vertical direction respectively. Among them, the downward stroke of flapping wing is taken as the start, the time phase represents the proportion of the leader in the whole flapping cycle when starting flapping, the positive value of the time phase represents that the leader lags behind the random, the flow direction distance between the two planes can be expressed by the flapping wavelength λ, and the spatial phase uses the time phase and wavelength λ, as shown in equation (1):

$$\phi_{spatial} = \phi_{temporal} - 2\pi\lambda \tag{1}$$

The zero spatial phase means that the leader and the follower flapping track are consistent, that is, the follower wingtip will flap along the front leader wingtip track. The positive value of the transverse distance Δ η indicates that there is overlap between the leading aircraft and the follower, while the

negative value refers to the distance away from the leading aircraft. (All of these parameters are shown in Figure 1 and normalized by chord length.)

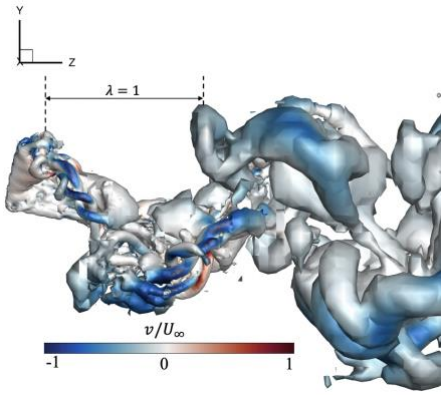

Figure 2 – The streamwise distance of an ornithopter during a flapping cycle is expressed in wavelength.

4. Results

In this section, the simulation of wing-vortex-interaction of flapping wing close formation under one variable is given. In these cases, in order to approach the cruise characteristics of the formation, the solution is advanced five times to eliminate the start-up related errors and establish the main periodic interaction. A total of more than 10 cycle times were simulated, and the phase average solutions of the last five flapping cycles were collected for subsequent analysis.

In order to match with the existing biological research and compare the conclusions, on the basis of ensuring the formation has a certain degree of close, according to the intensity decay of the vortex generated by the leader, we choose the flow direction distance of the two as half a wavelength, that is, according to Portugal's point of view, when the spatial phase is in phase, the temporal phase difference of the two aircrafts is π. In addition, according to the scaling law theory [15] of flapping wing fliers, the initial tip overlap of this model is set as $\Delta\eta_0 = 9.58\% \cdot b$. According to the development of flow structure and the level of aerodynamic load, the relationship between them and temporal phase will be explained respectively.

The purpose of this section is to explore the case of different temporal phase difference between two aircraft in flapping wing formation, and to understand the flow structure and unsteady aerodynamic load of flapping wing when encountering different incident vortices in the whole cycle. These five cases were compared with the leading birds flying solo. For the convenience of analysis (and verification of Portugal's conjecture that the V-shaped formation may have the potential best aerodynamic effect in the same phase), the variation range of the selected phase difference is $\phi_{temporal} = 0,\ \frac{\pi}{4},\ \frac{3\pi}{4},\ \pi,\ \frac{3\pi}{2}$, including the possible extensive conjecture and the completely opposite phase for further analysis and exploration.

The main phases of magnitude of a flapping cycle are shown in Figure 3, where phase (1) - phase (5) denotes the downward stroke, phase (5) - phase (8) denotes the upward stroke, and phase (1) and phase (5) denote that the wingtip is at the highest and lowest points respectively.

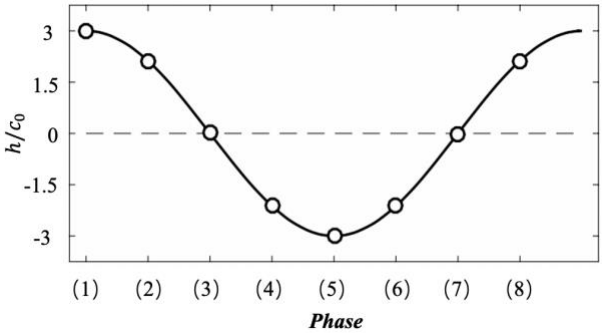

Figure 3 – phase distribution of wingtip trajectory.

4.1 Description of 3D flow structure

For the case of $\phi_{spatial} = 0, \phi_{temporal} = \pi$, the wingtip trajectories of the overlap sides of the leader and follower will match. This is also indicated by the vortex structure characterized by the Q-criterion [16] in Figure 4. The dotted line indicates the change caused by vortex interaction on the overlap side of the wing tip, and the opposite side (solid line) indicates that the vortex structure is basically symmetrical. Figure 5 shows the unsteady flow field evolution of the flapping wing formation through the Q-criterion iso-surface of phase change. The flow velocity coloring is used to distinguish the characteristics. Figure 5 (a) shows the front of the wing and (b) shows the back.

At the beginning of the downstroke (phase-1), it is interesting that there is an obvious difference in the TIV produced by the follower near the tip of the overlap side compared with that of the non-overlap side. Structurally, the complex coherent structure of the non-overlap side TIV is lost, and the vortex tube scale shrinks to a certain extent. Spatially, it does not follow the process of the wing tip downward flap, but to a large extent, it tends to the opposite direction of development (vertical positive direction). By observing the detailed evolution of flow structure at lower Q-value of Q-criterion, the LEV, TIV and TEV on the wing surface of the leading aircraft keep the same flow velocity as the free flow after shedding. Therefore, it can be inferred that the TIV with special structure on the overlap side of the follower is induced by the incident vortex (generated by the leader) at phase-1. On the lower side of the wing, compared with the non-overlap side, there is no horseshoe vortex structure on the overlap side, but an expansion structure on the trailing edge of the wing. As shown in Figure 6, the wing on the overlap side of the follower is in the upwash region just outside the incident vortex. It is inferred that the existence of upwash increases the effective angle of attack with random angle, which not only suppresses the flow separation on the lower surface of the wing, but changes the formation and evolution of the TIV.

Continue to flap down to phase-2, the upper surface of the wing produces obvious LEV. The high lift mechanism of leading-edge vortices was first discovered by Ellington [17], which shows that LEV can increase lift by adsorbing the attached vortex core on the upper surface of the leading-edge when the wing is flapping. Because of the rigid leading-edge has no deformation, the vortex core of the LEV in phase-2 attaches to the leading-edge and keeps parallel to the leading-edge of the wing. A low pressure region is generated on the suction side of the leading-edge and the wing generates lift. At phase-3, the leading-edge of the wing reaches the horizontal position. At this time, the LEV from the top of the downstroke to the middle begins to break into two parts, and a hollow is formed in the middle. As shown in Figure 8 (1), (2) and (3), the leading-edge vortex experienced a process of transient breakdown to reform, and the pressure on the wing surface increased briefly under the missing flow structure, while the low pressure distribution remained continuous before and after separation. The instability caused by the breakdown of LEV will cause buffeting on the flexible wing in this study (the specific effect on the aerodynamic load will be discussed in the next section) Description). At this time, the incident vortex is closer to the lower surface of the wing, and its induction is enhanced, which weakens the TEV on the overlap side (which can be clearly observed in the lower surface). It can be seen that the TIV formed by phase-1-4, LEV and the breakdown TEV near the trailing edge form a complex coherent vortex wake. Induced by the incident vortices on the overlap side, the spatial distribution of the vortices is changed, which shows that the overall vortex structure and vortex core begin to shift towards the negative vertical direction and the overlap side. Compared with the non-overlap side, it can be inferred that this is related to the weakening of TEV from phase-3, thus changing the coupling mechanism of vortices shedding from the overlap side. It can be seen from Figure 9 (phase-4 pressure iso-surface) that there is pinch-off of the incident vortex near the leading-edge tip of the overlap side and it continues until the end of the downstroke. The coupling of leading-edge vortices changes the formation and flow of TIV and TEV, and the lower surface of phase-5 wing (the red dotted circle) shown in Figure 10(a). In addition, the spatial drift of vortex core induced by the interaction between TIV and incident vortex can be observed in Figure 10(b).

At the upstroke, a new LEV is generated on the lower surface, and the LEV on the upper surface begins to break down and shed, accompanied by a new wing flow instability. It is worth noting that the formation and shedding of the LEV on both sides of the wing surface are obviously different between the down and up stroke (phase-2 and Phase-6). The former breaks down rapidly and connects with the structure on the upper surface to form a ring-shaped TEV, while the latter attaches to the upper surface continuously, and the size of the newly formed LEV on the lower surface is also

significantly smaller than that of the former. This kind of vortex structure distribution will lead to a huge difference in the vortex lift on both sides of the wing. In the downstroke, only the LEV on the upper surface will provide vertical vortex lift, while in the upstroke not only the strength of the LEV on the suction side is less than that on the upstroke, but also the LEV on the upper and lower surfaces will produce opposite adsorption force, which is reflected in the negative lift on the wing and will be partially offset. This phenomenon is reflected by the pressure distribution on the wing surface (Figure 6, pressure distribution of phase-5 and 6) and the lift curve in the next section. When flapping to the upstroke median (phase-7) shown in Figure 10(c), the LEV on the lower surface of the overlap wing breakdowns and the adsorption effect on the lower surface weakens. Compared with the downstroke median, the incident vortex is far away from the wing, and its scale is smaller, and its coupling with follower's TIV and LEV is weakened. At the end of the upstroke, the pressure distribution and the development of vortex structure on the overlap and non-overlap wing surfaces are symmetrical, so the influence of the incident vortex on the overlap wing surface is weakened at this stage. Combined with the upstroke and downstroke characteristics, it shows that there is a certain coupling relationship between the aerodynamic effect of the wing and the incident vortex and the intensity of the incident vortex, the distance between them and the time of keeping close.

Throughout the upstroke the scale of LEV and TIV of the leader and follower is significantly smaller than those of the downstroke, which leads to the decrease of the induction effect of the incident vortex on the follower, which is manifested in the vortex instability and spatial position drift. The reason for this phenomenon may be related to the setting of positive angle of attack and the geometric model of flapping wing. But in general, it does not change the characteristics of the interaction between the incident vortex and the wing when the spatial phase is in phase ($\phi_{spatial} = 0, \phi_{temporal} = \pi$) .

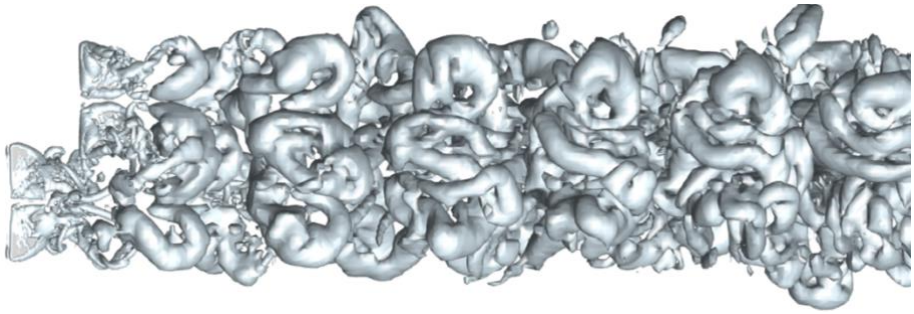

Fig 4 – Iso-surfaces of Q-criterion depicting the vortex wake on the upper surface of the wing.

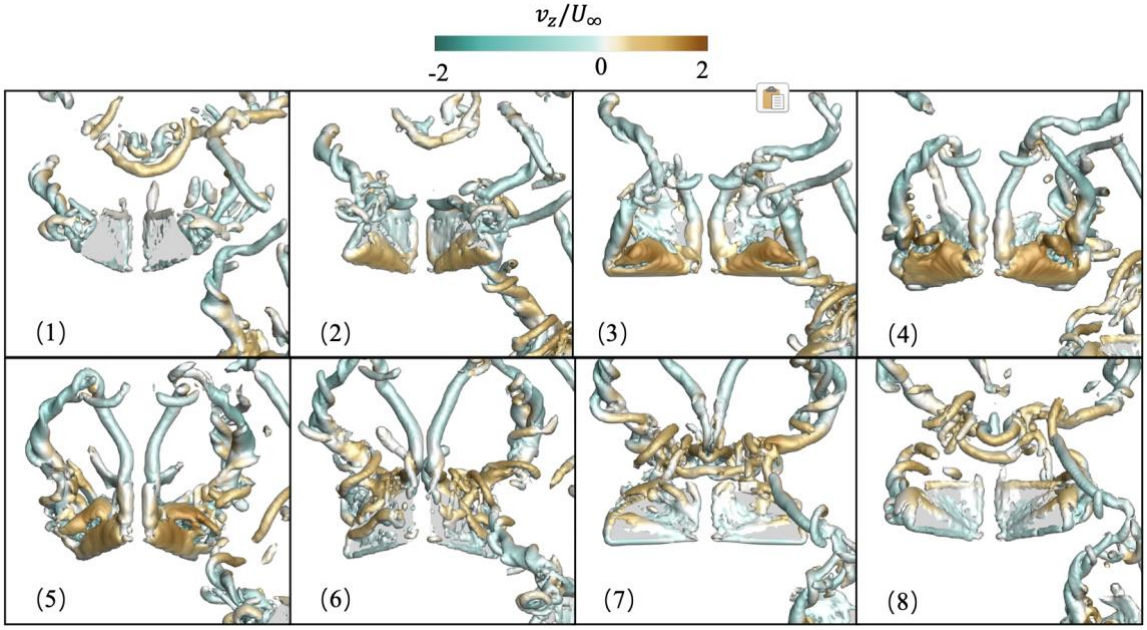

(a) Upper surface

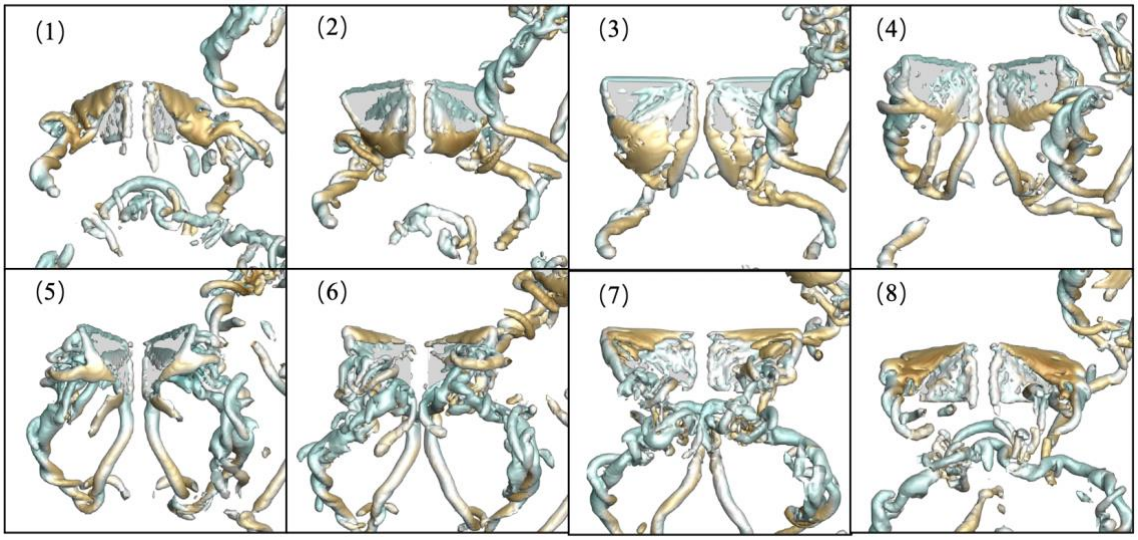

(b) Lower surface

Figure 5 – $\phi_{spatial} = 0$, $\phi_{temporal} = \pi$, Iso-surfaces of Q-criterion depicting the vortex structure of follower, colored by streamwise velocity

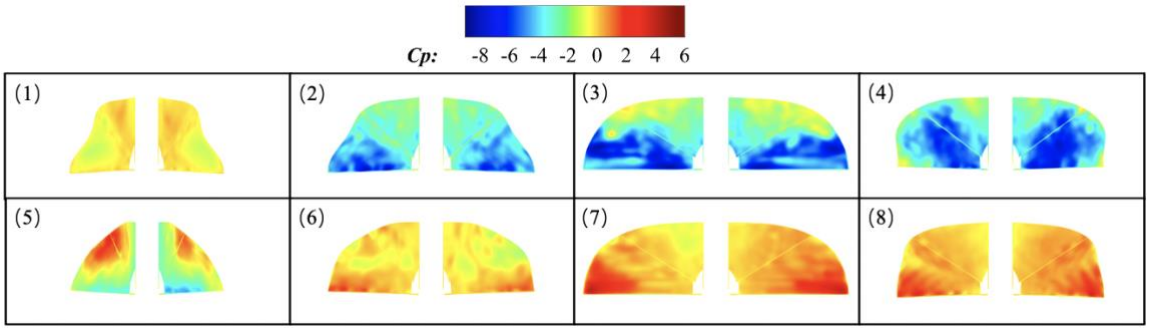

(a)upper surface

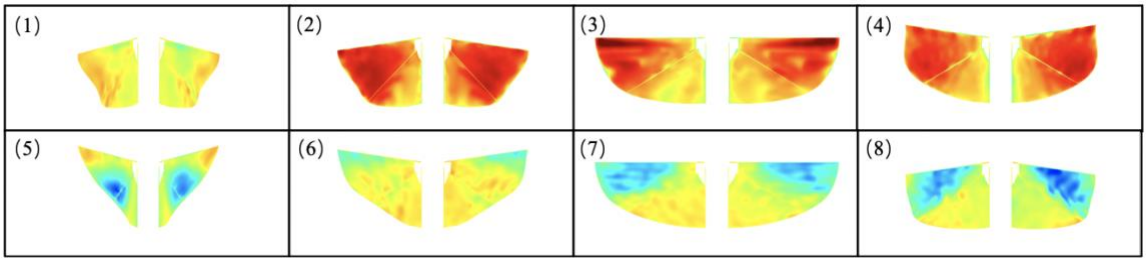

(b)under surface

Figure 6 – $\phi_{spatial} = 0$, $\phi_{temporal} = \pi$, Contours of instantaneous pressure coefficient on the (a) upper surface and (b) under surface.

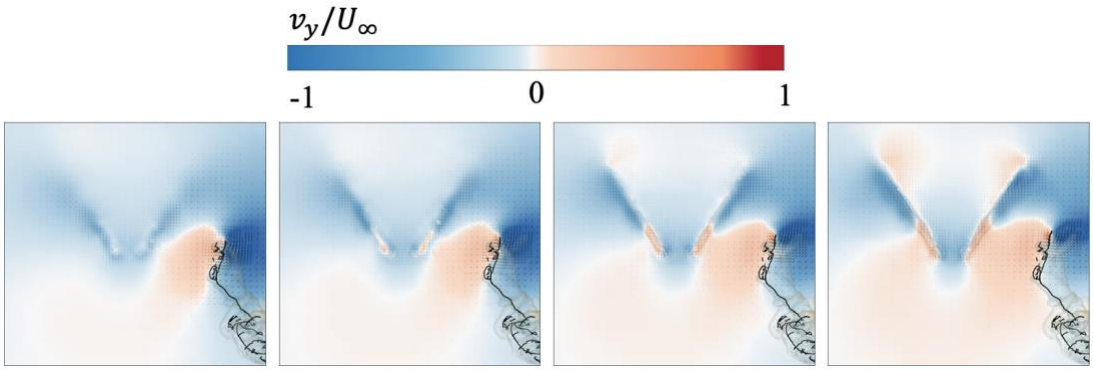

(a)Z = 0 (b) Z = 0.2C (c) Z = 0.4C (d) Z = 0.6C

Figure 7 – Slices of the vertical component of the flow, depicting the distribution of upwash and downwash flow near the leading-edge of phase-1.

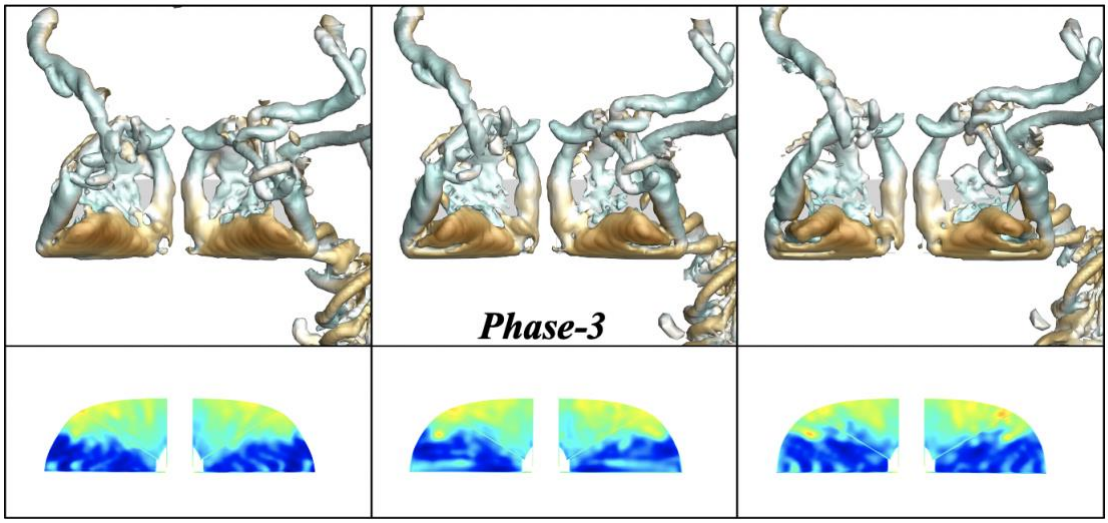

Figure 8 – Development of LEV near phase-3.

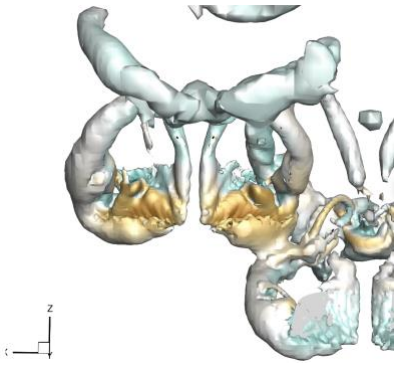

Figure 9 – Iso-surfaces of total pressure of phase-4.

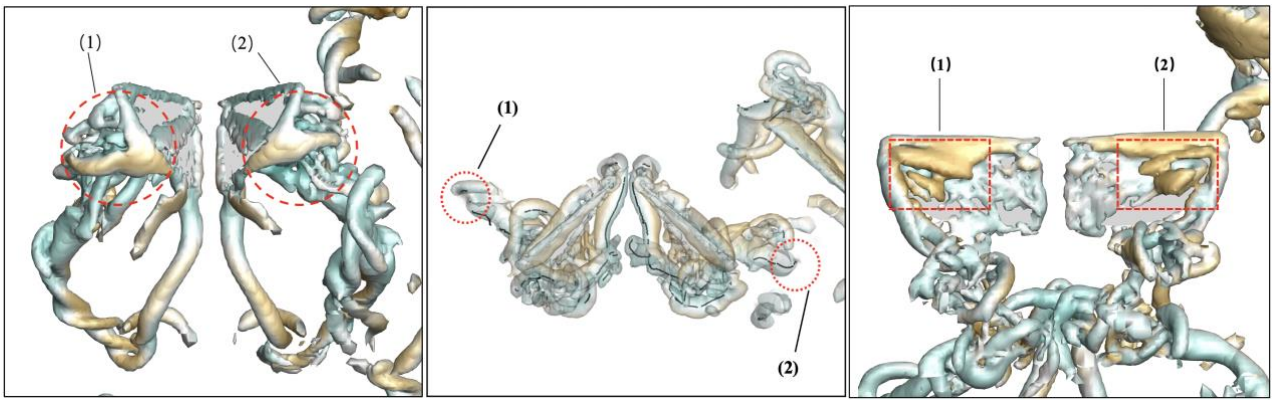

(a) (b) (c)

Figure 10 – Supplementary of phase-(5,7). (a) shows asymmetric flow structure on the lower surface. The black curve inside the vortex structure is the position of the vortex core. (b)The spatial drift of vortex core. The black curve inside the vortex structure is the position of the vortex core. The red circle in the figure B shows the shift of the TIV and the vortex core of the incident vortex. (c) shows the LEV breakdown on the overlap side of the lower surface for pahse-7.

The flow structure in other phases is similar to that in $\phi_{temporal} = \pi$, and the change of aerodynamic load is related to the flow structure correspondingly. Therefore, in order to highlight the difference of flow structure caused by the change of temporal phase, in the case of $\phi_{temporal} = \frac{\pi}{4}, \frac{3\pi}{4}$, the flow structure will be described only in the part where the difference is obvious from the solo flying aerodynamic load curve. The dimensionless time t/T in the range of 0 ~ 1 is used to characterize the different stages of the flow structure in the flapping cycle.

For temporal phase $\phi_{temporal} = \frac{\pi}{4}$, $\phi_{spatial} \neq 0$ is shown in Figure 11. When t/T = 0.2 (near phase-3), the trailing edge of the wing collides with the incident vortex, and the size of TEV on the overlap side decreases, and it begins to break down. Due to the wing buffeting caused by the breakdown of LEV near the downstroke median, the breakdown of TEV will have a complex coupling effect with this process on the wing surface. In the rest of the time, the overlap and non-overlap flow structures of the followers have relatively high symmetry, and the TIVs of the two sides are close in scale, and there is no obvious spatial drift. The above results show that the interaction phase(of a flapping cycle) between the incident vortex and the overlap wing is relatively concentrated in this temporal phase, and the induction effect on the formation and development of the follower vortex is weak in the whole cycle.

For temporal phase $\phi_{temporal} = \frac{3\pi}{4}$, $\phi_{spatial} \neq 0$ is shown in Figure 12. When t/T = 0.25 (near phase-3), the incident vortex is very close to the lower surface of the overlap wing. By observing the vertical velocity distribution of the leading-edge, we can know the distribution of the upwash and downwash of the incident vortex. As shown in Figure 12 (b), the downwash region from the middle of the leading-edge to the tip of the wing on the overlap side is induced by the incident vortex, resulting in the decrease of the vertical component of the air velocity (compared with the non-overlap side) and the effective angle of attack of the wing. When the flapping reaches t/T = 0.375 (phase-4), the incident vortex collides with the wing tip and merges with the follower's TIV, forming a spiral secondary vortex structure around them. On the other hand, the LEV on the upper surface of the overlap wing splits into two parts and forms a hollow at the fracture, which is similar to the breakdown of the LEV when the flapping wing is flapping to the middle of downstroke. Figure 14 shows that this change will enhance the adsorption effect on the upper surface and reduce the surface pressure near the wing tip on the lower surface.

According to the above flow structure analysis, it can be inferred that because the spatial distribution of the leading aircraft TIV (incident vortex) is consistent with the height of the wingtip trajectory, the periodic offset of the wingtip trajectory caused by the temporal phase may lead to collision or other complex interaction between the follower and incident vortices only in the finite time of the flapping cycle, or the difference between the induction and coupling interaction of vortices in $\phi_{temporal} = \pi, \phi_{temporal} \neq 0$.

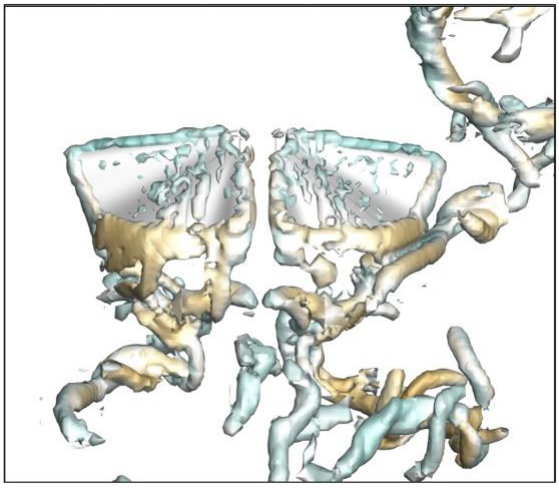

Figure 11 – $\phi_{temporal} = \frac{\pi}{4}$, t/T = 0.2, iso-surfaces of Q-criterion depicting the vortex structure, colored by streamwise velocity.

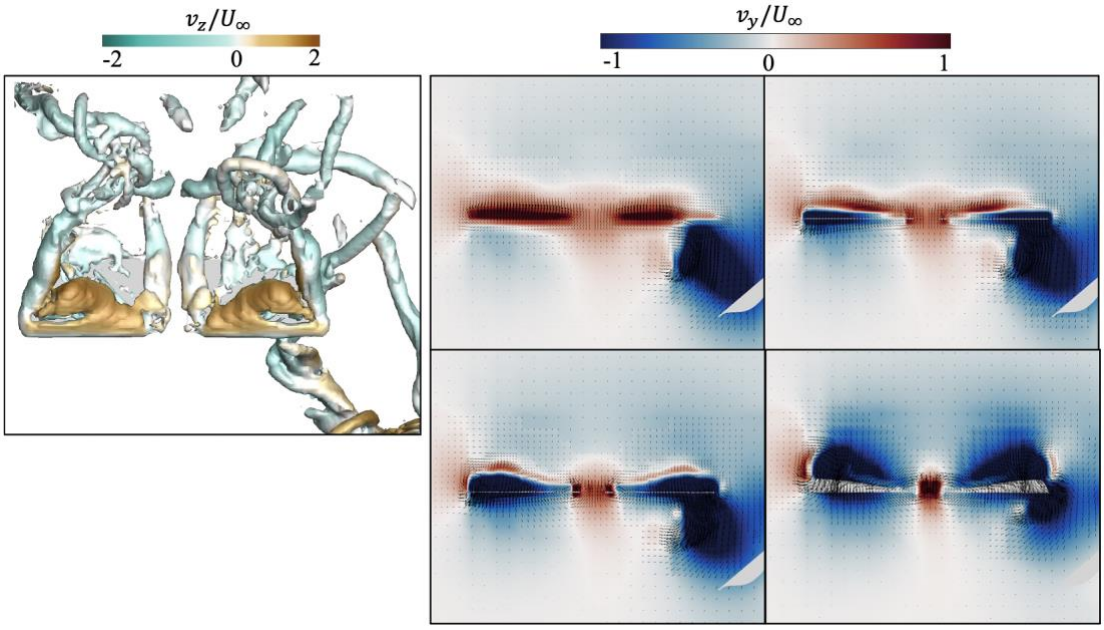

(a) Vortex structure (b) Upwash and downwash distributions

Figure 12 – $\phi_{temporal} = \frac{3\pi}{4}$, $phase - 3$, (a) Iso-surfaces of Q-criterion depicting the vortex structure, colored by streamwise velocity and (b) the slices at the leading-edge, colored by vertical velocity, describing the distribution of upwash and downwash.

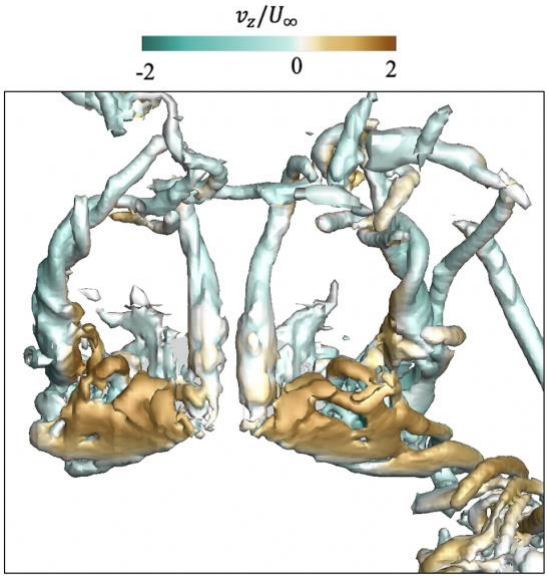

Figure 13 – $\phi_{temporal} = \frac{3\pi}{4}$, $phase - 4$ (t/T = 0.375), iso-surfaces of Q-criterion depicting the vortex structure, colored by streamwise velocity.

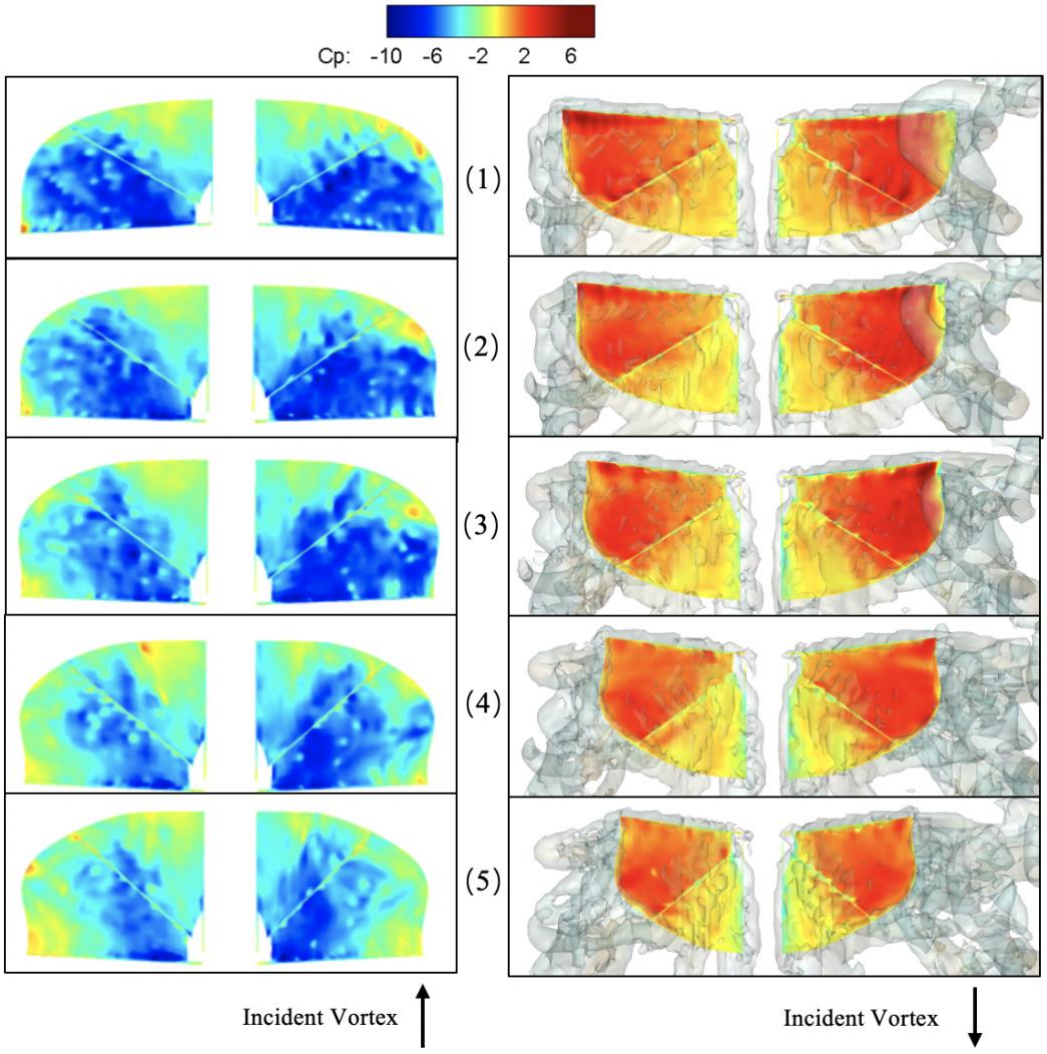

(a) Upper surface (b) Lower surface

Figure 14 – Surface pressure distribution near $\phi_{temporal} = \frac{3\pi}{4}$, t/T = 0.35. (3) denotes phase-4. Each number is in chronological order, with an interval of 1/40 of a flapping cycle

4.2 Aerodynamic load

Figure 15 shows the lift and thrust curves of the cycle average when the spatial phase of the follower and the leader are in phase ($\phi_{spatial} = 0, \phi_{temporal} = \pi$), which corresponds to the phase-1-8 of the flapping stroke.

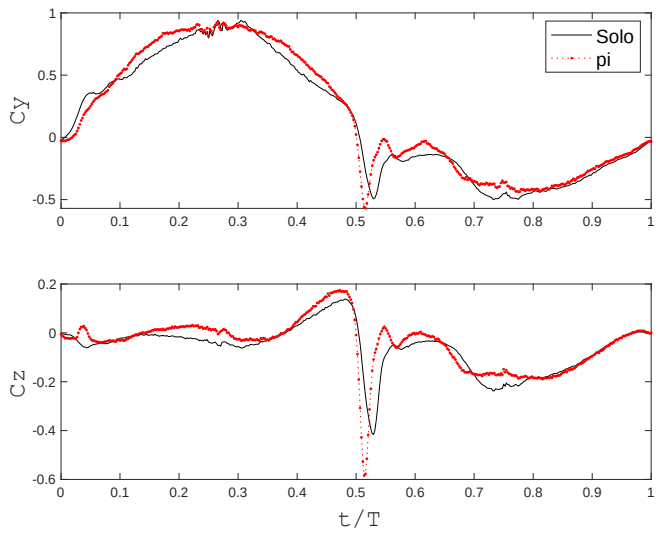

Figure 15 – Phase-averaged aerodynamic loads for $\phi_{spatial} = 0, \phi_{temporal} = \pi$

From the phase-3 vortex analysis in the previous section, it can be seen that the vortex breakdown instability (spiral mode instability) on the flexible wing surface may lead to buffeting of the flexible wing, and the aerodynamic load layer mainly shows that the phase averaged lift curve oscillates near the lift peak of T/T = 0.25 (phase-3). Compared with the curve of solo, the breakdown of LEV is the main contribution of the wing-vortex-interaction. At this time, the net thrust is negative, which shows drag, and solo shows thrust. The increasing trend of lift and drag is opposite with flapping. Near phase-5, the velocity of rigid leading-edge decreases to 0m/s^2 and begins to reverse, while the middle and part of trailing edge of flexible wing still keep flapping motion due to its own inertia and carbon fiber rod inertia. As a result, the wing undergoes a short stretch before it pours up, resulting in a sudden thrust increase, which is manifested in the peak of lift and thrust curve t/T = 0.5. As mentioned above, the asymmetry of the lower and upstroke LEV results in the obvious difference of the aerodynamic load curve in a period of time. The negative lift is offset by the LEV on the upper and lower surfaces of the upstroke, which is shown in the "depression" of the lift curve t/T = 0.530-0.625 (corresponding to a period of time near Phase-6). And the peak value of negative lift is less than that of positive lift. Compared with solo, the induced effect of the incident vortex is reflected in the change of lift and thrust amplitude and the oscillation of the curve between t/T = 0.5 and 0.625. Near the median of upstroke (phase-7), the breakdown of overlap LEV is observed, which shows the decrease of negative lift near t/T = 0.75.

The curves of lift and thrust period average of different temporal phases are shown in Figure 16 (a). It can be seen that t/T = 0~0.1 except for $\phi_{temporal} = \pi$, the other temporal phases are consistent with solo in terms of lift and thrust. For $\phi_{temporal} = \pi$, the main difference between the aerodynamic load curve and solo is that the lift near the center of downward flutter is larger, and it is inferred that the main reason is the breakdown of TEV. In the case of $\phi_{temporal}$=3π/4, the lift near the median of the downthrow stroke (t/T = 0.25) is less than that of solo. According to Figure 12 (b) in the previous section, it can be seen that the downwash flow of the incident vortex reduces the effective AOA near the overlap wing tip, resulting in the decrease of lift. In the process of t/T = 0.35~0.45, the increase of lift is due to the change of surface pressure on the overlap wing caused by the breakdown of LEV.

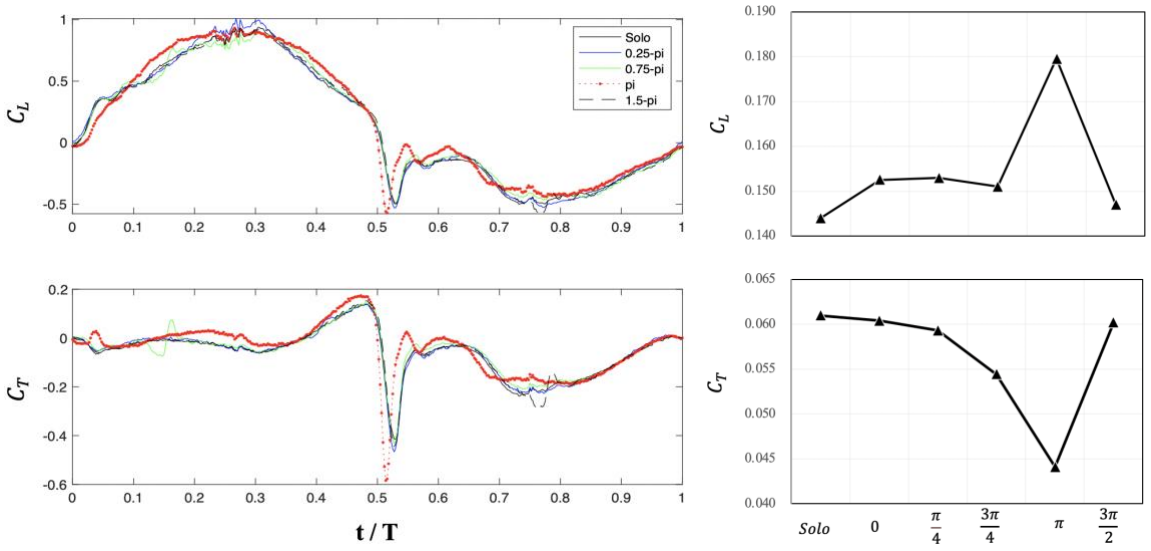

(a)Phase-averaged (b)Time-mean

Figure 16 – Aerodynamic loads for different temporal phase in (a) phase-averaged and (b)time-mean

Figure 16 (b) shows the relationship between mean lift—thrust and temporal phase. When the fixed the distance of wingtip overlap ($\Delta\eta_0$) is selected, the average lift keeps a certain degree of increase under the action of the incident vortex, reaches the peak in $\phi_{temporal} = \pi$ and decreases on both sides. The lift is positively correlated with the phase difference distance π. In other words, when the spatial phase of the two aircraft is in phase, the interaction between the incident vortex and the

overlap wing has the greatest effect on the follower's lift, while the net thrust is opposite. The specific promotion is shown in table 1. To some extent, the distribution curve shows that when only changing the time phase relationship, the aerodynamic effect of flapping wing close formation has the optimal coupling of lift, that is, when the leader and the random are in phase in space, the average lift is the highest, and the average net thrust is the lowest.

Table 1

		Solo	0	$\frac{\pi}{4}$	$\frac{3\pi}{4}$	π	$\frac{3\pi}{2}$
C_L	Value	0.144	0.153	0.153	0.151	0.180	0.147
	% diff	—	5.91	6.22	4.88	24.66	2.13
C_T	Value	0.061	0.060	0.059	0.054	0.044	0.060
	% diff	—	-1.00	-2.69	-10.76	-27.69	-1.30

5. Conclusion

In this paper, the fluid structure interaction (FSI) of flapping wings in close formation is studied by using the LBM method and the finite element method. The compact V-shape configuration of thin film flapping wing at half wavelength distance and Reynolds number Re = 20000 is studied.

In order to understand the flow structure and potential unsteady sources in aeroelastic response, this work studies the aerodynamic effects of different phase differences between two aircraft with rigid leading-edge and flexible wing. Through the observation of convective structure in several cases, it is shown that the vortex dynamics changes a lot when the streamwise vortices (incident vortices) generated by the leader pass through the follower. First of all, due to the alternate flapping, the distribution of the induced flow direction on both sides of the incident vortex is also periodic. Therefore, when the incident vortex does not collide with the wing, the effective angle of attack on one side of the wake will change in the upwash or downwash region of the incident vortex. It is mainly manifested in restraining flow separation, generating secondary vortex structure, accelerating the breakdown of vortex on surface of wing and changing the mechanism of vortex shedding. These changes will lead to complex wing vortex interaction.

When the heading position of the two aircraft is fixed, the number of spatial wavelengths is determined, so the spatial phase of the two aircraft is determined. When the spatial phases are in phase ($\phi_{temporal} = 0$), the non-overlap vortex wake of the two aircraft flapping is almost symmetrical in space, and the velocity of the vortex wake of the leader is consistent with that of the free flow. Therefore, the follower is flapping along the "path" of the leader. As the incident vortex approaches the follower's TIV, the vertical and spanwise drift of the core is induced. The two vortex will keep close to each other and move synchronously, and the incident vortex will not collide with the wing. When the tip vortex of a flapping wing has difference in spatial phase ($\phi_{temporal} \neq 0$), the periodic phase difference caused by the tip trajectory of the two aircraft leads to the collision between the wing and the incident vortex or other effects at a specific time. In this case, the action time and effect of the incident vortex are much weaker than those of the former.

In addition, the unsteady vortex dynamics caused by the complex vortex wing interaction generated by the flexible flapping wing itself is also worthy of attention. Due to the setting of positive angle of attack, a larger size of LEV is formed on the wing near the leading-edge during downstroke, which leads to stronger adsorption effect on the suction side, which is manifested in the surface pressure on the suction side during downstroke and upstroke. During the upstroke, LEV will be formed on both sides of the wing surface, which will weaken the generation of negative lift during the upswing. Near the median of upstroke and downstroke, the LEV will break into two parts in streamwise, causing strong buffeting of the flexible wing, which is reflected in the fluctuation and peak of the aerodynamic load curve.

By comparing the aerodynamic loads under different phases, it can be concluded that the aerodynamic effect of the close formation configuration of flapping wing, which is set according to the statistical conclusions of the existing fixed wing and flapping wing organisms, shows the increase of lift and the decrease of net thrust. When the spatial phase is in the same phase, the aerodynamic

effect is obviously different from other cases with spatial phase difference, and the maximum lift is achieved. In other cases, the aerodynamic load lift decreases on both sides of the phase. This may explain to some extent the aerodynamics of the preference of flapping wing aircraft or biological v-formation for phase.

6. Contact Author Email Address

Mailto: zhaolf@buaa.edu.cn

7. Copyright Statement

References

[1] Lissaman, B. and Shollenberger, A. Formation flight of birds. *Science*, Vol. 168, No. 3934, pp. 1003-1005,1970.

[2] Garmann D, Visbal M. Interactions of a streamwise-oriented vortex with a finite wing. *Journal of Fluid Mechanics,* vol. 767, pp 782-810, 2015.

[3] Iglesias S. and Mason H. Optimum Span loads in Formation Flight, *AIAA Paper 2002-1358*, Reno, NV, 2002.

[4] Triantafyllou S, Yue P. Hydrodynamics of Fishlike Swimming, *Ann. Rev. of Fluid Mechanics,* 32: 33-53, 2000.

[5] Ginevsky S, Zhelannikov I. Vortex wakes of Aircrafts. *Springer,* Berlin Heidelberg, 2009.

[6] Usherwood R, Stavrou M, Lowe C, et al. Flying in a flock comes at a cost in pigeons. *Nature*, Vol. 474, No. 7352, pp 494-7, 2011.

[7] Weimerskirch H., Martin J., Clerquin Y., Alexandre, P. and Jiraskova S. Energy saving in flight formation. Nature 413, 697-698, 2001.

[8] Portugal J, Hubel Y, Fritz J, Heese S, Trobe D, Voelkl B, Hailes S, Wilson M. and Usherwood R. Upwash exploitation and down- wash avoidance by flap phasing in ibis formation flight. *Nature,* Vol. 505, 399-404, 2014.

[9] Portugal Steve. Lissaman, Shollenberger and formation flight in birds. *Journal of Experimental Biology*, Vol. 219, No. 18, pp 2778-2780, 2016.

[10] Barnes J, Visbal R and Gordnier E. Analysis of streamwise-oriented vortex interactions for two wings in close proximity. *Physics of Fluids*, Vol. 27, No. 1, pp 261-278, 2015.

[11] Wagner G, Jacques D , Blake W , et al. Flight Test Results of Close Formation Flight for Fuel Savings. *AIAA Journal*, 2002.

[12] Dogan A, Venkataramanan S, and Blake W. Modeling of Aerodynamic Coupling Between Aircraft in Close Proximity. *Journal of Aircraft*, Vol.42, No. 4, pp 941–955, 2005.

[13] Blake B, and Gingra R. Comparison of Predicted and Measured Formation Flight Interference Effects. *Journal of Aircraft*, Vol. 41, No. 2, pp 201–207, 2004.

[14] Taylor K, Nudds L, Thomas R. Flying and swimming animals cruise at a Strouhal number tuned for high power efficiency. *Nature,* Vol. 425, pp 707–711, 2003.

[15] McMasters J and Henderson M. Low speed single element airfoil synthesis. *Technical Soaring*, Vol. 6, pp. 1–21, 1980.

[16] Jeong J, Hussain F. On the identification of a vortex. *Journal of Fluid Mechanics*, Vol. 332, No. 1, pp 339-363, 1995.

[17] Ellington C P, Berg C V D, Willmott A P, and Thomas A L R. Leading-edge vortices in insect flight. *Nature*, Vol. 384, pp 626–630, 1996.